

# Electronic and magnetic properties of Si substituted Fe<sub>3</sub>Ge

K. V. Shanavas,<sup>a)</sup> Michael A. McGuire, and David S. Parker

Materials Science and Technology Division, Oak Ridge National Laboratory, Oak Ridge, Tennessee 37831-6056, USA

(Received 19 July 2015; accepted 10 September 2015; published online 23 September 2015)

Using first principles calculations, we studied the effect of Si substitution in the hexagonal Fe<sub>3</sub>Ge. We find the low temperature magnetic anisotropy in this system to be planar and originating mostly from the spin-orbit coupling in Fe-*d* states. Reduction of the unitcell volume reduces the magnitude of in-plane magnetic anisotropy, eventually turning it positive which reorients the magnetic moments to the axial direction. Substituting Ge with the smaller Si ions also increases the anisotropy, potentially enhancing the region of stability of the axial magnetization, which is beneficial for magnetic applications such as permanent magnets. Our experimental measurements on samples of Fe<sub>3</sub>Ge<sub>1-x</sub>Si<sub>x</sub> confirm these predictions and show that substitution of about 6% of the Ge with Si increases by approximately 35 K the temperature range over which anisotropy is uniaxial. © 2015 AIP Publishing LLC. [<http://dx.doi.org/10.1063/1.4931574>]

## I. INTRODUCTION

The iron rich intermetallic compounds Fe-Sn, Fe-Ge, etc., and their alloys have been of interest because of their potential applications in permanent magnets and magnetic refrigeration.<sup>1,2</sup> The binary system Fe<sub>3</sub>Ge, in particular, is a good ferromagnet with Fe moments of  $2.0 \mu_B$  at room temperature and a Curie temperature of  $T_c = 640$  K.<sup>3</sup> However, the magnetization is planar at low temperatures and the system undergoes a spin-reorientation transition at  $T_{SR} = 380$  K, beyond which the moments are aligned along the *c* axis. Partial substitution of Fe with Mn was found to reduce the spin-reorientation transition to lower temperatures while also reducing saturation magnetization.<sup>4</sup> Applied pressure, on the other hand, enhances the axial region of magnetization without affecting the magnetic moments.<sup>4</sup>

In the present manuscript, we study the electronic structure to understand the origin of magnetic properties of Fe<sub>3</sub>Ge with the help of first principles calculations. We find that the magnetic anisotropy originates from the Fe-*d* states and that reduction in the unitcell volume reduces the in-plane anisotropy. This leads to the possibility of improving the magnetic properties by replacing Ge with smaller ions such as Si, since a continued reduction in planar anisotropy may ultimately lead to uniaxial anisotropy useful for permanent magnets. Subsequently, samples of pure and Si doped Fe<sub>3</sub>Ge are prepared and characterized which confirm the reduction in spin-reorientation transition temperature by Si substitution, extending the temperature range over which the magnetic anisotropy is uniaxial.

## II. METHODS

*Theoretical:* The first principles calculations are carried out within density functional theory (DFT) as implemented in VASP code,<sup>5</sup> using projector augmented waves<sup>6</sup> and generalized gradient approximation. An energy cutoff of 450 eV

and *k* space sampling on a  $17 \times 17 \times 18$  grid are found sufficient to get converged results. The magnetic anisotropy energy is obtained by calculating the total energies of the system with magnetic moments pointing along *a* and *c* directions with spin-orbit coupling and using the expression,  $K_u = E\{\hat{a}\} - E\{\hat{c}\}$ . Partial doping of Ge site with Si is realized by virtual crystal approximation.

*Experimental:* Diffraction and microstructural analysis of stoichiometric Fe<sub>3</sub>Ge samples indicated the composition that forms under the conditions employed here is near Fe<sub>77</sub>Ge<sub>23</sub> (Fe<sub>3.08</sub>Ge<sub>0.92</sub>), consistent with literature reports. To examine the effects of Si substitution for Ge, samples of Fe<sub>77</sub>Ge<sub>23</sub> and Fe<sub>77</sub>Ge<sub>20.7</sub>Si<sub>2.3</sub> were prepared. For the Si-doped sample, Ge<sub>0.9</sub>Si<sub>0.1</sub> was first prepared by arc-melting. Iron powder was mixed thoroughly with Ge powder or Ge<sub>0.9</sub>Si<sub>0.1</sub> powder in an agate mortar and pestle. Samples were pressed into pellets, sealed in silica tubes with 0.3 atm ultra-high-purity Ar, and placed into a furnace preheated to 900 °C. After 20 h at this temperature, the samples were quenched in ice water. X-ray diffraction from the surface of the pellets was collected with a PANalytical Xpert Pro diffractometer and analyzed to determine phase purity and lattice parameters using the HighScore Plus software package from PANalytical.

## III. RESULTS

The stable phase of Fe<sub>3</sub>Ge has a face-centered-cubic (L1<sub>2</sub>, space group *Fm* $\bar{3}$ *m*) structure which transforms to a hexagonal (DO<sub>19</sub> with space group *P*6<sub>3</sub>/*mmc*) above 700 K.<sup>7</sup> Due to the slow formation kinetics of the fcc phase, the hexagonal phase is easily preserved upon cooling to room temperatures. We focus on the hexagonal phase in this study, since cubic materials usually have very low magnetic anisotropy and hence little potential as hard magnetic materials. The unitcell of this phase of Fe<sub>3</sub>Ge is shown in Fig. 1. It consists of hexagonal planes of Fe along the *c* axis, with 25% of the atoms replaced with Ge.

<sup>a)</sup>Electronic mail: kavungalvees@ornl.gov

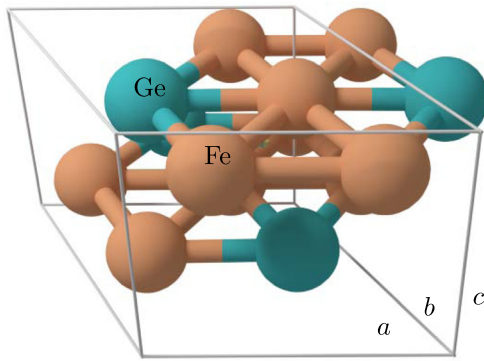


FIG. 1. Crystallographic unit cell of the hexagonal phase of  $\text{Fe}_3\text{Ge}$  consists of hexagonal planes of Fe along the  $c$  axis with 25% replaced with Ge. There are two formula units per cell.

The Fe-Si binary compound  $\text{Fe}_3\text{Si}$ , on the other hand, is stable only in the cubic phase.<sup>8</sup> However, we expect that the alloy  $\text{Fe}_3\text{Ge}_{1-x}\text{Si}_x$  will be stable in the hexagonal structure for small values of  $x$ .

### A. First-principles calculations

The electronic structure of  $\text{Fe}_3\text{Ge}$  is summarized in the spin polarized density of states plots shown in Fig. 2. The states near the Fermi level are predominantly of Fe- $d$  character with completely full spin-up states and approximately three electrons in spin down states per Fe atom. There is an exchange splitting of about 3 eV, although the distribution of the states in the up and down spin-channel is quite different suggesting asymmetric hopping parameters for the two channels. The Fe- $4s$  states are empty, whereas Ge- $4s$  are fully occupied (around  $-9$  eV in Fig. 2). The Ge- $4p$  states are substantially spread out in energy and counting the number of occupied states, we estimate the valence configuration of Ge to be  $s^2p^2$ . These results point to an electronic configuration of Fe- $d^8$  and a magnetic moment of  $2\mu_B$ . The moments

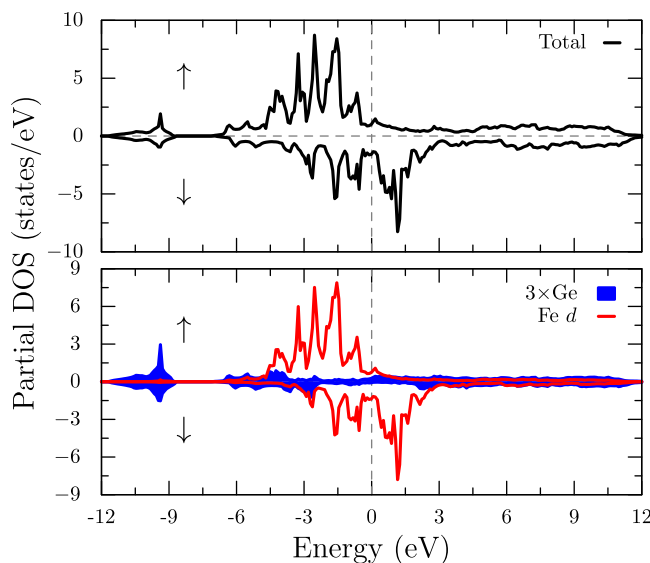


FIG. 2. Total and partial spin polarized density of states per formula unit for  $\text{Fe}_3\text{Ge}$  in the ferromagnetic configuration. Positive and negative DOS values correspond to spin-up and spin-down states, respectively. The Fermi level is set to 0 eV.

calculated from spin-polarized charge densities in a sphere of radius  $1.3 \text{ \AA}$  around the Fe atoms give a moment of  $2.15 \mu_B$ , which is reasonably close to the value calculated from DOS. The net magnetization is  $M = 1.27 \times 10^6 \text{ A/m}$  ( $M = 6.42 \mu_B/\text{f.u.}$  or 1.6 T) and compares reasonably well with the experimental value of  $M_s^{5K} = 1.14 \times 10^6 \text{ A/m}$  listed in Table I.

In the relaxed structure which has volume of  $96.2 \text{ \AA}^3$ , we find a magnetic anisotropy of  $K_1 = -0.103 \text{ meV/f.u.}$  or  $K_1 = -0.35 \text{ MJ/m}^3$  which compares reasonably well with our experimental value of  $K_1 = -0.5 \text{ MJ/m}^3$  deduced from the magnetization data in Fig. 4(a). The negative sign means that the moments prefer to align in the  $ab$  plane. By individually turning off the spin-orbit coupling at Fe and Ge sites and calculating the magnetic anisotropy energy, we find that 74% of the contribution to  $K_1$  arises from the Fe sites. From the calculated  $K_1$  as a function of volume, plotted in Fig. 3(a) for  $\text{Fe}_3\text{Ge}$  we show that compression increases  $K_1$ , eventually making it positive. As the red circles show, the substitution of Ge with Si reduces the equilibrium volume of the material, leading to near zero magnetic anisotropy energy (MAE) for 50% Si doping and positive MAE for  $\text{Fe}_3\text{Si}$ . For fixed volume, the magnetic anisotropy increases with Si doping, suggesting that the lower spin-orbit coupling of Si and the change in crystal field also affects the MAE in this system.

The calculated variation of the magnetic anisotropy energy at 0 K, as a function of Si doping in  $\text{Fe}_3\text{Ge}$  is plotted in Fig. 3(b). We optimized the  $\text{Fe}_3\text{Ge}$  structure in the ferromagnetic configuration at each Si concentration and find that doping decreases volume as expected. From the figure, we can see that the anisotropy becomes axial above Si doping levels of 0.6. The magnetic moments are in-plane at lower doping levels but are weaker than pure  $\text{Fe}_3\text{Ge}$ . Thus, even small Si doping is beneficial since a weaker in-plane anisotropy at 0 K will tend to lower the spin-reorientation transition temperature, potentially improving the room temperature coercivity.

In Fig. 3(a), we see that the magnetic anisotropy also increases when volume is increased from its equilibrium

TABLE I. Experimental results from pure and partially silicon substituted  $\text{Fe}_3\text{Ge}$ , including composition measured by EDS, lattice parameters ( $a$ ,  $c$ ,  $V$ ) and density ( $\rho$ ) from x-ray diffraction at room temperature, and measured saturation magnetization ( $J_s$ ,  $M_s$ ) at 300 and 5 K. Note  $J = \mu_0 M$  and  $1 \text{ T} = 10^4 \text{ G}$ .

Nominal composition	$\text{Fe}_{77}\text{Ge}_{23}$	$\text{Fe}_{77}\text{Ge}_{20.7}\text{Si}_{2.3}$
Measured composition	$\text{Fe}_{77(1)}\text{Ge}_{23(1)}$ $\text{Fe}_{3.1}\text{Ge}_{0.9}$	$\text{Fe}_{77(1)}\text{Ge}_{22(1)}\text{Si}_{1.3(2)}$ $\text{Fe}_{3.1}(\text{Ge}_{0.94}\text{Si}_{0.06})_{0.9}$
$a$ ( $\text{\AA}$ )	5.1779(2)	5.1713(2)
$c$ ( $\text{\AA}$ )	4.2242(2)	4.2172(2)
$c/a$	1.226	1.226
$V$ ( $\text{\AA}^3$ )	98.08	97.67
$\rho$ ( $\text{g/cm}^3$ )	8.075	8.028
$T_{SR}$ (K)	383	312–319
$T_C$ (K)	627	595
$J_s^{300K}$ (T)	1.35	1.36
$M_s^{300K}$ (A/m)	$1.07 \times 10^6$	$1.08 \times 10^6$
$J_s^{5K}$ (T)	1.44	1.47
$M_s^{5K}$ (A/m)	$1.14 \times 10^6$	$1.17 \times 10^6$

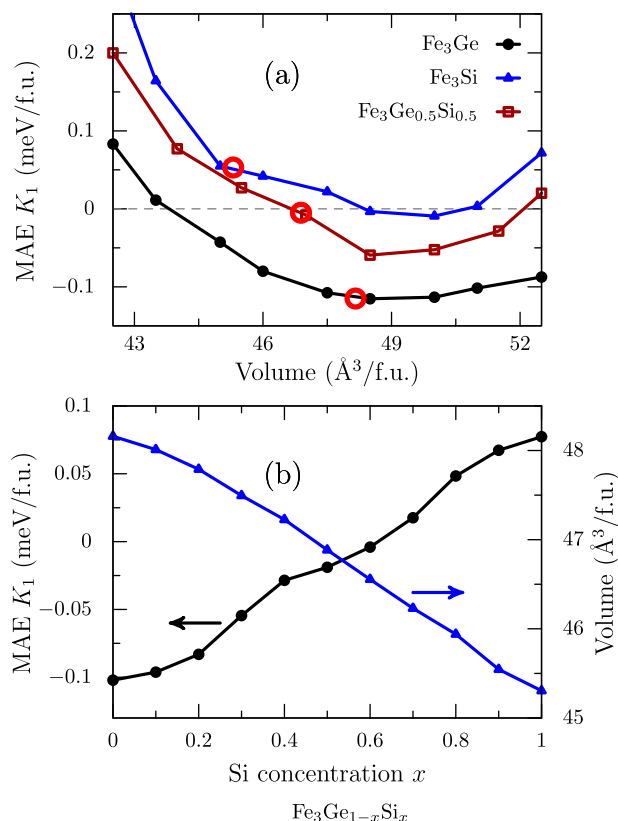


FIG. 3. Variation of magnetic anisotropy energy (MAE)  $K_1$  calculated (a) as a function of volume of the unitcell for  $\text{Fe}_3\text{Ge}$ ,  $\text{Fe}_3\text{Si}$  and  $\text{Fe}_3\text{Ge}_{0.5}\text{Si}_{0.5}$  and (b) as a function of Si concentration  $x$  in  $\text{Fe}_3\text{Ge}_{1-x}\text{Si}_x$  with relaxed volume at each concentration. The relaxed volumes (blue curve) are plotted in the right axis of (b). Red circles in (a) correspond to the ambient pressure volume of each phase.

value. This suggests that the thermal expansion leads to the experimentally observed increase in  $K_1$  upon heating,<sup>4</sup> which is consistent with other transition metal magnets that undergo spin-reorientation transition such as  $\text{MnBi}$ .<sup>9</sup> However, the contribution from thermal expansion is small in  $\text{Fe}_3\text{Ge}$  and hence, the lattice phonons may also play an important role in the spin reorientation transition in this system.<sup>10</sup>

## B. Experimental measurements

The  $\text{Fe}_{77}\text{Ge}_{23}$  sample was phase pure with all observed Bragg reflections indexed to the  $\text{Mn}_3\text{Cd}$ -type structure (space group  $P6_3/mmc$ ) as shown in Fig. 4(c). A single, small, and unindexed impurity reflection was observed in the  $\text{Fe}_{77}\text{Ge}_{20.7}\text{Si}_{2.3}$  sample, with the rest indexed to  $\text{Mg}_3\text{Cd}$  structure-type. The intensity of the impurity peak was 2% of the intensity of the strongest peak from the target phase. Refined unit cell parameters are shown in Table I. The chemical composition of the samples was investigated using a Hitachi T3000 tabletop SEM, with a Bruker Quantax 70 energy dispersive x-ray detector. The composition of the  $\text{Fe}_3\text{Ge}$ -like phase was determined by averaging measurements on eight separate grains. Results are shown in Table I. The results show that the silicon content in the target phase (6%) is lower than that in the loaded composition (10%). Silicon and oxygen rich inclusions were observed,

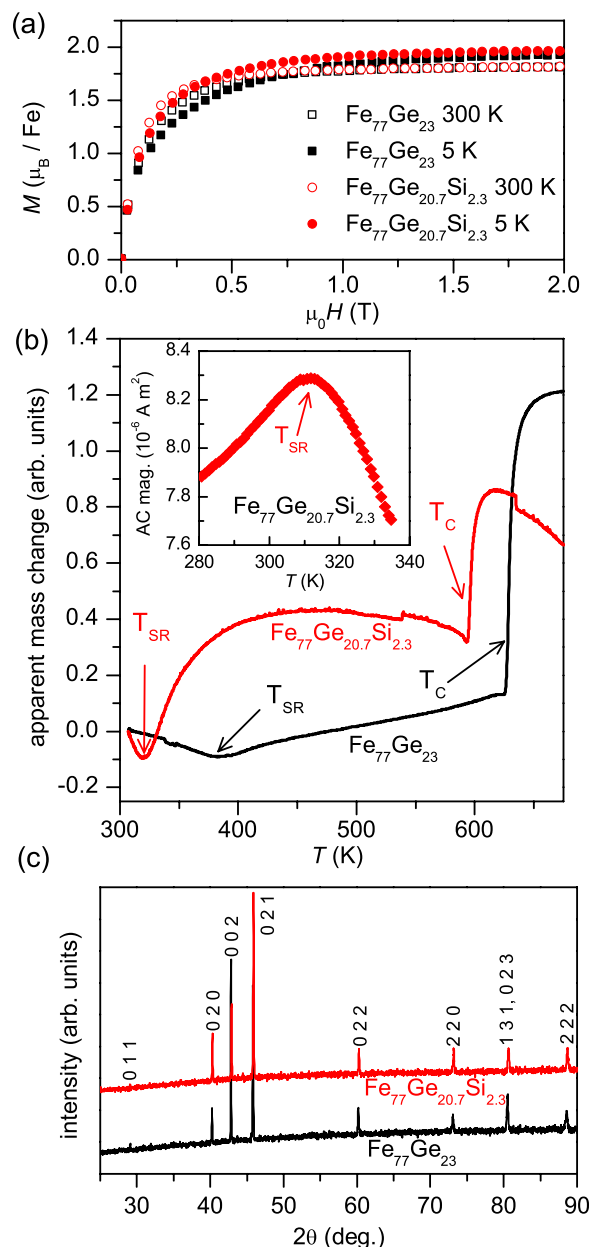


FIG. 4. Magnetic measurement results for samples of nominal composition  $\text{Fe}_{77}\text{Ge}_{23}$  and  $\text{Fe}_{77}\text{Ge}_{20.7}\text{Si}_{2.3}$ . (a) Isothermal magnetization curves used to determine saturation magnetization. (b) Thermogravimetric data measured in the presence of a weak magnetic field opposing gravity, used to detect magnetic phase transitions manifested as changes in the apparent mass of the sample. The inset in (b) shows AC magnetization data collected in zero DC field near the spin reorientation temperature in the Si-doped sample.

suggesting that this may make up the balance of the silicon; however, some of this may have originated from the silica tube wall.

Isothermal magnetization measurements were performed on the polycrystalline samples at 300 and 5 K using a Physical Property Measurement System (Quantum Design). Data are shown in Fig. 4. Saturation magnetizations are reported in Table I. Spin-reorientation and Curie temperatures were determined by thermogravimetric analysis performed in the presence of a weak magnetic field gradient, so that changes in the magnetic force on the sample were observed as changes in the apparent mass (Fig. 4).

AC magnetization measurement performed in zero applied DC field was also used to detect the spin-reorientation temperature in the Si doped sample. This measurement gave a result (312 K) close to but slightly lower than that obtained from the thermogravimetric analysis (319 K). The experimental results show that the effect of 6% Si substitution is to decrease  $T_C$  by 32 K and  $T_{SR}$  by 70 K, extending the range over which axial magnetic anisotropy is observed while having little effect on the size of the moment.

#### IV. CONCLUSIONS

Our theoretical calculations and experimental measurements suggest that Si doping in the intermetallic compound  $\text{Fe}_3\text{Ge}$  is beneficial to the room temperature magnetic properties of this system. In the hexagonal phase at 0 K, the system is strongly ferromagnetic with magnetic moments of  $2.15 \mu_B$  per Fe and the magnetic anisotropy is in-plane with  $K_1 = -0.1 \text{ meV/f.u.}$  We find that both a compressive strain and substitution of the Ge atoms by Si weaken the planar anisotropy energy. A larger magnetic anisotropy constant  $K_1$  at zero temperature can extend the region of stability of the axial magnetization and potentially bring the reorientation transition below room temperature. The calculated anisotropy at 0 K is found to become axial upon doping with Si above 60%. Our experimental measurements with small Si concentrations confirm these predictions; we find the spin-reorientation temperature drops from 383 K to below 320 K when doped with 6% Si, indicating an enhanced stability of the axial phase as predicted by the calculations. It is plausible that higher Si substitution levels would further lower the spin-reorientation temperature, leading to useful uniaxial anisotropy at room temperatures.

#### ACKNOWLEDGMENTS

Work at Oak Ridge National Laboratory was supported by the Critical Materials Institute, an Energy Innovation Hub funded by the U.S. Department of Energy, Energy Efficiency and Renewable Energy, Advanced Manufacturing Office (K.V.S. and D.P.) and U.S. Department of Energy, Office of Energy Efficiency and Renewable Energy, Vehicle Technologies Office, Propulsion Materials Program (M.A.M.).

- <sup>1</sup>B. C. Sales, B. Saparov, M. A. McGuire, D. J. Singh, and D. S. Parker, "Ferromagnetism of  $\text{Fe}_3\text{Sn}$  and alloys," *Sci. Rep.* **4**, 7024 (2014).
- <sup>2</sup>L. Zhang, E. Brück, O. Tegus, K. J. Buschow, and F. de Boer, "The crystallographic phases and magnetic properties of  $\text{Fe}_2\text{MnSi}_{1-x}\text{Ge}_x$ ," *Physica B* **328**, 295 (2003).
- <sup>3</sup>J. W. Drijver, S. G. Sinnema, and F. v. d. Woude, "Magnetic properties of hexagonal and cubic  $\text{Fe}_3\text{Ge}$ ," *J. Phys. F: Met. Phys.* **6**, 2165 (1976).
- <sup>4</sup>F. Albertini, D. Negri, L. Pareti, E. B. Watts, Z. Arnold, J. Kamarad, G. Calestani, A. Deriu, and S. Besseghini, "Magnetocrystalline anisotropy of  $\text{Fe}_3\text{Ge}$  single crystal: Effect of pressure and Mn substitution for Fe," *J. Appl. Phys.* **96**, 2110 (2004).
- <sup>5</sup>G. Kresse and J. Hafner, "Ab-initio molecular dynamics for liquid metals," *Phys. Rev. B* **47**, 558 (1993); G. Kresse and J. Furthmüller, "Efficient iterative schemes for *ab initio* total-energy calculations using a plane-wave basis set," *ibid.* **54**, 11169 (1996).
- <sup>6</sup>P. E. Blöchl, "Projector augmented-wave method," *Phys. Rev. B* **50**, 17953 (1994).
- <sup>7</sup>Q. Z. Chen, A. H. W. Ngan, and B. J. Duggan, "The  $L_{12} \leftrightarrow DO_{19}$  transformation in the intermetallic compound  $\text{Fe}_3\text{Ge}$ ," *J. Mater. Sci.* **33**, 5405 (1998).
- <sup>8</sup>M. Schütte, R. Wartchow, and M. Binnewies, "Shape controlling synthesis formation of  $\text{Fe}_3\text{Si}$  by the reaction of iron with silicon tetrachloride and crystal structure refinement," *Z. Anorg. Allg. Chem.* **629**, 1846 (2003).
- <sup>9</sup>V. P. Antropov, V. N. Antonov, L. V. Bekenov, A. Kutepov, and G. Kotliar, "Magnetic anisotropic effects and electronic correlations in MnBi ferromagnet," *Phys. Rev. B* **90**, 054404 (2014).
- <sup>10</sup>K. V. Shanavas, D. Parker, and D. J. Singh, "Theoretical study on the role of dynamics on the unusual magnetic properties in mnbi," *Sci. Rep.* **4**, 7222 (2014).